Available online at www.sciencedirect.com
SCIENCE DIRECT®
Biochemical and Biophysical Research Communications 322 (2004) 168–176
BBRC
www.elsevier.com/locate/ybbrc

Expression of zebrafish glutamate receptor δ2 in neurons with cerebellum-like wiring

Yoshinori Mikami, Tomoyuki Yoshida, Naoto Matsuda, Masayoshi Mishina*

Department of Molecular Neurobiology and Pharmacology, Graduate School of Medicine, University of Tokyo, Japan
SORST, Japan Science and Technology Agency, Tokyo 113-0033, Japan

Received 28 June 2004
Available online 3 August 2004

Abstract

Mammalian glutamate receptor (GluR) δ2 is selectively expressed in cerebellar Purkinje cells and plays key roles in cerebellar plasticity, motor learning, and neural wiring. Here, we isolated cDNA encoding the zebrafish ortholog of mammalian GluRδ2. We found that in adult zebrafish brain, *glurδ2* mRNA was expressed not only in cerebellar Purkinje cells, but also in the crest cells of the medial octavolateral nucleus (MON) and the type I neurons of the optic tectum. Immunohistochemical analysis revealed that zebrafish GluRδ2 proteins were selectively localized in the apical dendrites of these neurons. Interestingly, the crest cells of the MON and the type I neurons of the optic tectum receive large numbers of parallel fiber inputs at the apical dendrites and sensory inputs at the proximal or basal dendrites. These results suggest that the expression of zebrafish GluRδ2 is selective for cerebellum-like neural wiring with large numbers of parallel fiber inputs.

Keywords: Apical dendrite; Cerebellar Purkinje cell; Crest cell of the medial octavolateral nucleus; Glutamate receptor δ2; Neural wiring; Parallel fiber; Type I neuron of the optic tectum; Zebrafish

Glutamate receptor (GluR) channels play a key role in fast excitatory synaptic transmission, synaptic plasticity, higher brain function including learning and memory, and synapse refinement during brain development. Based on the pharmacological and electrophysiological properties, GluR channels have been classified into three major subtypes that are the α-amino-3-hydroxy-5-methyl-4-isozaxole propionic acid (AMPA), kainate, and *N*-methyl-D-aspartate (NMDA) receptors [1]. Molecular cloning studies revealed the presence of 18 GluR channel subunit genes, which can be classified into seven subfamilies based on the amino acid sequence identities [2,3]. Six of them well correspond to the pharmacologically defined subtypes. We found GluRδ subtype as a novel member of GluR channel family by molecular cloning [4]. With respect to the amino acid sequence identity, GluRδ subtype is positioned between the NMDA and non-NMDA subtypes. GluRδ2, the second member of GluRδ subfamily, is selectively expressed in Purkinje cells of the cerebellum [5,6], and within cerebellar Purkinje cells, GluRδ2 proteins are localized at the postsynaptic density (PSD) of the parallel fiber-Purkinje cell synapses, but not at the climbing fiber-Purkinje cell synapses [7,8]. GluRδ2 mutant mice showed impairments in long-term depression (LTD) at the parallel fiber-Purkinje cell synapse [9], motor learning [10,11], stabilization of the parallel fiber-Purkinje cell synapse [9,12], and refinement of climbing fiber innervation to Purkinje cells [9,13,14]. However, it remains a mystery how GluRδ2 regulates cerebellar synaptic plasticity and parallel fiber synapse formation. GluRδ1 and GluRδ2 expressed in *Xenopus* oocytes or mammalian cells failed to form functional channels. The carboxyl-terminal of GluRδ2

* Corresponding author. Fax: +81 3 5841 3570.
E-mail address: mishina@m.u-tokyo.ac.jp (M. Mishina).

0006-291X/$ - see front matter © 2004 Elsevier Inc. All rights reserved.
doi:10.1016/j.bbrc.2004.07.095

associates with PSD-95/Dlg/ZO-1 (PDZ)-domain containing proteins including PTPMEG and Delphilin [15,16]. Recently, we found a novel interaction of GluRδ2 with Shank proteins through an internal motif [17]. Furthermore, GluRδ2, Shank1, Shank2, Homer, metabotropic glutamate receptor 1α (mGluR1α), and glutamate receptor interacting protein (GRIP) 1 formed a postsynaptic signaling complex, suggesting that through Shank1 and Shank2, GluRδ2 can interact with the mGluR1, AMPA receptor, and inositol 1,4,5-triphosphate receptor type 1 (IP_3R1) that are essential for cerebellar long-term depression.

Zebrafish (*Danio rerio*) is an excellent model organism to investigate vertebrate brain development and function because transparent embryos and mutagenesis techniques facilitate phenotype-driven forward genetic analyses [18]. Recently, we developed a reverse genetic technique in zebrafish [19–21]. The neuron- and stage-specific expression of both effector and reporter molecules in combination with in vivo observation of a single neuron in living zebrafish embryos will provide a useful tool for the elucidation of molecular mechanisms underlying synapse formation and synapse dynamics. As an initial step to investigate how GluRδ2 regulates cerebellar synaptic plasticity and parallel fiber synapse formation by molecular genetic approaches in zebrafish, we here cloned the zebrafish ortholog of mammalian GluRδ2. Zebrafish and mammalian GluRδ2 proteins shared high amino acid sequence identity and showed conservation of several characteristic domains common to ionotropic GluRs. We found that in adult zebrafish brain, *glurδ2* was expressed not only in the cerebellar Purkinje cells, but also in the crest cells of MON and the type I neurons of the optic tectum. GluRδ2 proteins in these neurons were localized at the apical dendrites receiving large numbers of parallel fibers. These findings suggest the selective expression of zebrafish GluRδ2 in specific types of neurons with cerebellum-like neural wiring.

Materials and methods

Animals. The zebrafish AB strain was used. Zebrafish of the AB strain were raised and kept under the standard conditions at ~28 °C [19].

Cloning of zebrafish glurδ2 cDNA. A *glurδ2* cDNA fragment was amplified by a nested PCR on a cDNA library from adult zebrafish using 5′-TGCAGGAAGCATGCGAGTTG-3′ and 5′-TT(C/T)TTNG GCCACCA(C/T)TT(A/G)TG-3′ (N, four nucleotides) as primers for the first PCR and 5′-AGCCTTGGTCAGTTCTATCGG-3′ and 5′-CCACCANGCNCCCATCATCA-3′ as primers for the second PCR. The 1.6-kb cDNA fragment was cloned into pCRII (Invitrogen, Carlsbad, CA) to yield pCRII-zfGluRδ2-mid. The entire coding sequence of *glurδ2* was obtained using a SMART RACE cDNA Amplification kit (Clontech, Palo Alto, CA) with primers 5′-TGTTTTCCAGCTTTCGATCG-3′, 5′-ACAGCACCGTGTCGTAT ATG-3′, and 5′-CTCTGTTCATCAACTCGCATGC-3′ for 5′-RACE and primers 5′-TGGACTTCACCACCCGCTAC-3′ and 5′-CTCCA TGTGGTTTGTCTACG-3′ for 3′-RACE. The 0.8-kb 5′ and 1.6-kb 3′ cDNA fragments were cloned into pCRII to yield pCRII-zfGluRδ2-5 and pCRII-zfGluRδ2-3, respectively.

The nucleotide sequences of cDNA clones were determined on both strands using the ABI Prism BigDye Terminator Cycle sequencing ready reaction kit (PE Applied Biosystems, Foster City, CA) and were deposited in the DDBJ/EMBL/GenBank databases under Accession No. AB154207. The deduced amino acid sequences of zebrafish, mouse, and human GluRδ2 were aligned using GENETYX-MAC Ver.11.1 (Software Development, Tokyo, Japan) and ClustalW (DDBJ, Mishima, Japan) multiple alignment computer programs. Contig search was performed using BLAST algorithm at the Ensemble Zebrafish Genome Server website featuring the zebrafish whole genome shotgun assembly sequence version 3 (Sanger Institute, http://www.ensembl.org/Danio_rerio/).

3D structure modeling. A 3D structure of the GluRδ2 leucine/isoleucine/valine-binding protein (LIVBP)-like domain was modeled by homology to the structure of the unliganded form of LIVBP (Protein Data Bank (PDB) coordinates, 2LIV) on the basis of the sequence alignment among zebrafish GluRδ2, LIVBP, and leucine-binding protein (LEUBP: PDB coordinates, 2LBP). The 3D–1D alignment was performed by LIBRA I (DDBJ: http://www.ddbj.nig.ac.jp/E-mail/libra/LIBRA_I.html). The structural modeling was performed with the SwissPDBViewer (Swiss Institute of Bioinfomatics, Geneva, Switzerland; http://www.expasy.org/spdbv) [22].

In situ hybridization. Adult zebrafish were anesthetized on ice. Brains were fixed with the skull bone in Bouin (15 ml Van Gieson solution P (Wako, Osaka, Japan), 5 ml of 37% formaldehyde, and 1 ml acetic acid) at 4 °C overnight. The fixed zebrafish brains were carefully removed from the skull and dehydrated in graded ethanol, embedded in paraffin, and sectioned at 10 μm. All sections were mounted on glass slides precoated with MAS (Matsunami, Osaka, Japan).

The 1.6-kb *Eco*RI fragment from pCRII-zfGluRδ2-mid was subcloned into the pSPT18 to yield pSPT18-zfGluRδ2-mid. Digoxigenin (DIG)-11-UTP-labeled sense and antisense RNA probes specific for the zebrafish *glurδ2* gene were synthesized in vitro with T7 and SP6 RNA polymerases using *Hin*dIII- and *Pvu*II-cleaved pSPT18-zfGluRδ2-mid, respectively, using a DIG RNA Labeling Kit (Roche, Mannheim, Germany). Paraffin sections were deparaffinized and rehydrated. They were treated with 0.2 N HCl for 20 min and partially digested with 1 μg/ml proteinase K in 100 mM Tris–HCl (pH 8.0) and 50 mM EDTA at 37 °C for 10 min. Sections were fixed with 4% paraformaldehyde at room temperature for 20 min, acetylated with 0.25% acetic anhydride in 0.1 M triethanolamine–HCl at room temperature for 15 min, and prehybridized at 60 °C for 2 h in a prehybridization buffer containing 50% formamide, 0.02% Ficoll, 0.02% polyvinylpyrrolidone, 0.02% bovine serum albumin, 2× standard saline citrate (SSC; 150 mM NaCl and 15 mM sodium citrate), 10 mM EDTA, 100 μg/ml tRNA (Sigma, St. Louis, MO), and 0.01% Tween 20. Hybridization was performed at 60 °C for 12 h in the prehybridization buffer supplemented with 5% dextran sulfate and 0.25–1 μg/ml DIG-labeled cRNA nucleotide probes. The slides were washed three times at 60 °C for 30 min in 2× SSC containing 50% formamide and 0.01% Tween 20, treated with 10 μg/ml RNase A at 37 °C for 1 h in 10 mM Tris–HCl (pH 8.0) containing 1 mM EDTA and 0.5 M NaCl, washed in 2 × SSC and 0.01% Tween 20 at 55 °C for 30 min, and washed twice in 0.1× SSC and 0.01% Tween 20 at 55 °C for 30 min. The hybridization reaction was visualized with DIG Nucleic Acid Detection Kit, using nitroblue tetrazolium as a purple chromogen (Roche).

Double labeling. The in situ hybridization for zebrafish *glurδ2* mRNA was visualized with HNPP (2-hydroxy-3-naphthoic acid-2′-phenylanilide phosphate) Fluorescent Detection Set, using HNPP/FastRed TR (4-chloro-2-methylbenzenediazonium hemi-zinc chloride salt) complex (Roche). After hybridization, sections were incubated with mouse anti-frog muscle parvalbumin antibody (1:2000; Sigma) at 4 °C overnight. For immunofluorescence they were incubated at room temperature with biotinylated anti-mouse IgG for 1 h and then with

avidin, Alexa Fluor 488 conjugate (Invitrogen) for 30 min. Sections were imaged by a confocal microscope (MRC-2100, Bio-Rad, Hercules, CA) with argon and/or helium–neon lasers using a Planapo 20× objective lens (Nicon, Tokyo, Japan).

Western blot analysis. Whole-brain homogenates were prepared from adult zebrafish and wild-type and GluRδ2 mutant mice as described [23]. Proteins (40 μg) were separated by SDS–PAGE and electroblotted onto a nitrocellulose membrane (Schleicher & Schuell, Dassel, Germany). After blocking with 5% skim milk in phosphate-buffered saline with 0.1% Tween 20 (PBST), the blots were incubated with rabbit anti-mouse GluRδ2 antibody [5] for 1 h at room temperature. The membrane was washed with PBST and incubated with a horseradish peroxidase-conjugated anti-rabbit IgG (1:1000; Amersham Biosciences, Piscataway, NJ) in PBST for 1 h at room temperature. The horseradish peroxidase was visualized using ECL Western blotting detection reagents (Amersham Biosciences). For a control, anti-GluRδ2 antibody was preabsorbed for 1 h at 20 °C with 100 μg/ml mouse GluRδ2 peptide.

Immunohistochemistry. Paraffin sections were incubated with rabbit anti-mouse GluRδ2 or GluRδ2-peptide-absorbed control antibody (1:10000) at 4 °C overnight. They were incubated at room temperature with biotinylated anti-rabbit IgG for 1 h at room temperature, and then with peroxidase-conjugated streptavidin for 30 min at room temperature, using a Histofine SAB-PO(R) kit (Nichirei, Tokyo, Japan). Immunoreaction was visualized with 3,3′-diaminobenzidine.

Results

Molecular characterization of zebrafish GluRδ2

From a zebrafish cDNA library, we isolated a cDNA fragment by PCR with degenerate primers based on the sequences of mouse, rat, and human *glurδ2* cDNAs [5,6,24]. The entire coding sequence of zebrafish *glurδ2* was obtained by 5′- and 3′-RACE. The deduced amino acid sequence shared 82%, 81%, and 81% identity with mouse, rat, and human GluRδ2, respectively. The amino acid sequence identity of zebrafish GluRδ2 with mammalian GluRδ1 was ~54% and those with mammalian AMPA-, kainate-, and NMDA-subtypes of GluR were ~26%, ~27%, and ~25%, respectively [2,3]. By BLAST searches of zebrafish *glurδ2* cDNA sequences against Sanger zebrafish genomic sequence project database, we found that *glurδ2* sequence was scattered on nine contigs. Using mouse GluRδ2 sequence, we found two additional contigs (chunk2229 and chunk6235) with high homology. Deduced amino acid sequences from these contigs shared 73–74% and 48–54% identity with mouse GluRδ1 and GluRδ2, respectively. Thus, we conclude that the cloned cDNA encodes the GluRδ2 ortholog of zebrafish. The zebrafish *glurδ2* gene was mapped on chromosome (Chr) 8 close to *atonal homolog 1* (*atoh1*) using the mapping panels of the Zebrafish Information Network (ZFIN: http://zfin.org/). Similarly, mammalian *Glurδ2* and *Atoh1* genes resided at the neighboring positions on human Chr 4q22 [24,25] and mouse Chr 6 [25,26]. The zebrafish *glurδ2* gene consisted of 16 exons and exon–intron boundaries were conserved between zebrafish and mouse *glurδ2* genes.

Fig. 1A shows the alignment of zebrafish, mouse, and human GluRδ2 amino acid sequences. Zebrafish GluRδ2 protein had characteristic features common to those of mammalian ionotropic GluRs such as the long amino-terminal domain, four hydrophobic stretches corresponding to channel-forming M2 and membrane-spanning M1, M3, and M4 segments, and the carboxyl terminus [2]. Notably, segment M2 (residues 587–605) is completely conserved among zebrafish and mammalian GluRδ2 [5,6,24]. The complete conservation implies the functional significance of M2 segment, possibly as the ion channel-forming or oligomerization domain. There is a high degree of conservation in segments M1 and M3 (95% identity). The segment 1 (S1) of lysine/arginine/ornithine-binding protein (LAOBP)-like domains [27] is also well conserved among species (91% identity). Alanine at position 638 is also conserved, the site of lurcher mutation that transforms GluRδ2 to a constitutively active channel [26]. The juxtamembrane segment (residues 838–865) important for plasma membrane targeting [28] and the S segment (residues 892–921) essential for the interaction with Shank proteins [17] are highly conserved (89% and 90% identity, respectively). Complete conservation is found for the carboxyl-terminal 10 amino acid residues (residues 984–993) involved in the PDZ domain recognition.

In addition, BLOSUM62 [29] scoring revealed the conservation in N1 (residues 53–73) and N2 (residues 312–351) segments of the amino-terminal leucine/isoleucine/valine-binding protein (LIVBP)-like domain [30] and in a proline-rich segment (residues 950–977) of the carboxyl-terminal region (Figs. 1A and B). We constructed a 3D structure model of the LIVBP-like domain of zebrafish GluRδ2 based on the homology to the unliganded form of bacterial LIVBP [31]. The modeled structure consisted of two globular lobes, each lobe being made of alternation of β strands and α helices, interconnected by a hinge made of three short linkers delineating a deep central cleft (Fig. 1C). The N1 and N2 segments are located on the surface of a globular domain corresponding to the N-domain of bacterial LIVBP that has the L-leucine-binding site.

Distribution of glurδ2 mRNA in the adult brain

We examined the expression patterns of zebrafish *glurδ2* mRNA in the adult brain by in situ hybridization using sagittal sections. The cerebellum showed strong hybridization signals (Figs. 2A and D). In addition, we found clear hybridization signals in the medial octavolateral nucleus (MON) (Figs. 2A and J) and the optic tectum (Figs. 2A and M). By 4 days postfertilization, *glurδ2* hybridization signals were detectable in the larval cerebellum.

In the cerebellum, the *glurδ2* hybridization signals were localized in the Purkinje cell layer of the lateral

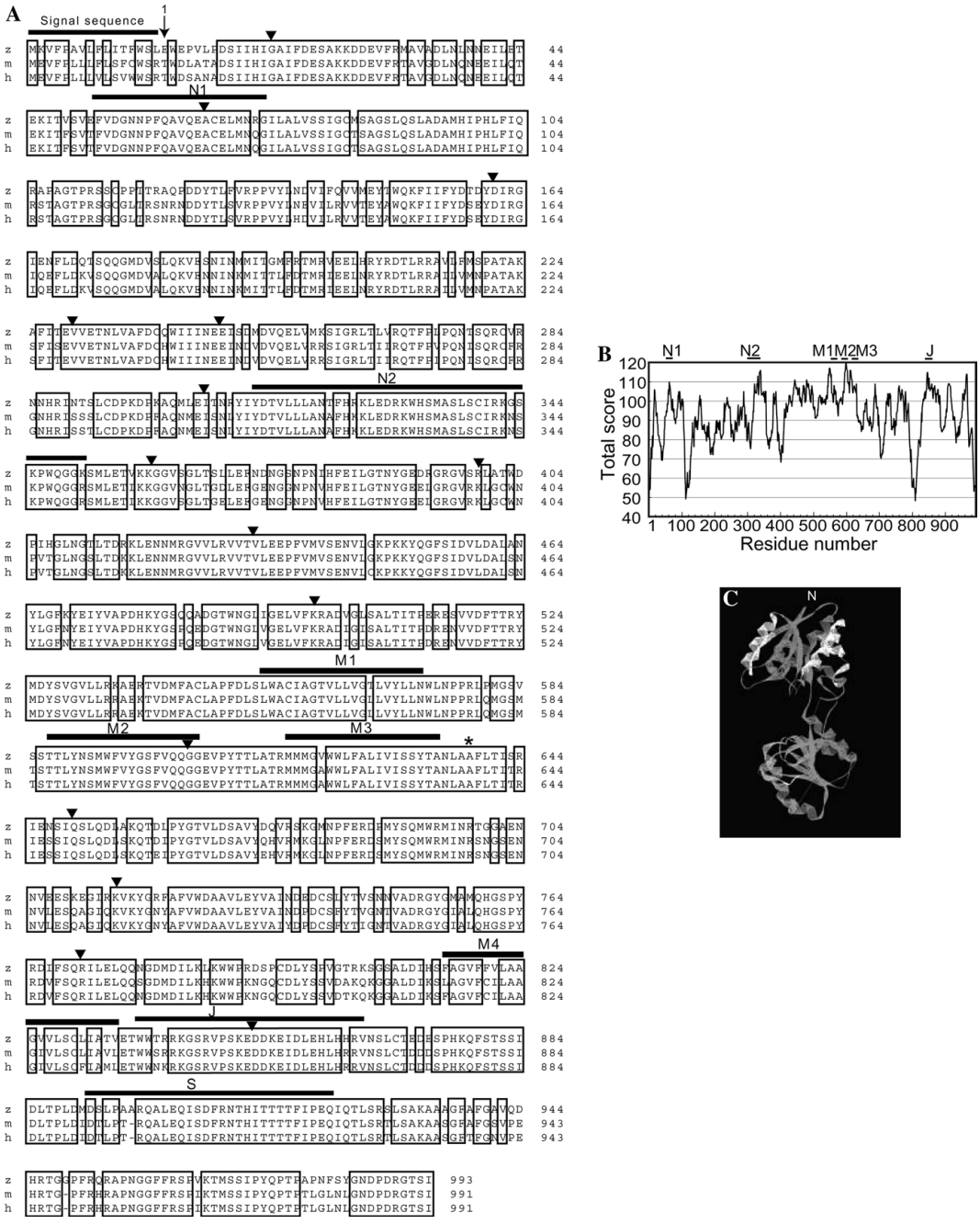

Fig. 1. Structural characterization of zebrafish GluRδ2. J, juxtamembrane segment; M1–M4, hydrophobic segments; N1, N2, conserved amino-terminal segments; and S, S segment. (A) Alignment of the deduced amino acid sequence of zebrafish (z) GluRδ2 with the mouse (m) and human (h) orthologs. The single amino acid code is used. Amino acid residues are numbered beginning with the amino-terminal residue of the proposed mature protein ([3], indicated by an arrow). Numbers of the amino acid residues are given at the right-handed ends of the individual lines. Sets of identical amino acid residues are shown in open boxes. Arrowheads indicate the junctions of exons, which are conserved among species. An asterisk marks the conserved alanine residue, the site of lurcher mutation. (B) Homology between zebrafish and mouse GluRδ2 proteins. The vertical axis gives the total BLOSUM62 score for residues in a 21-residue sliding window. (C) A 3D model of the LIVBP-like domain of GluRδ2 produced by homology modeling using the sequence alignment and the Protein Data Bank coordinates of LIVBP (2LIV). The well-conserved N1 and N2 segments are shown in white.

division of valvula cerebelli (Val), the medial division of valvula cerebelli (Vam), and the corpus cerebelli (CCe) (Figs. 2A and D). We double-labeled sagittal paraffin sections for *glurδ2* mRNA and parvalbumin protein, a good marker for Purkinje cells in the teleost cerebellum (Figs. 2F–H) [32]. The anti-parvalbumin antibody labeled dendrites, cell bodies, and axon terminals of Purkinje cells in the valvula cerebelli (Va) and in rostral and caudal parts of CCe (Fig. 2G), while little signals were detectable in the dorsal region. All

immunoreactive signals for parvalbumin protein in Purkinje cell bodies (green, Fig. 2G) were well merged with hybridization signals for *glurδ2* mRNA (red, Fig. 2F) in the Va and CCe (Fig. 2H). In the cerebellum, zebrafish *glurδ2* mRNA was thus selectively expressed in Purkinje cells.

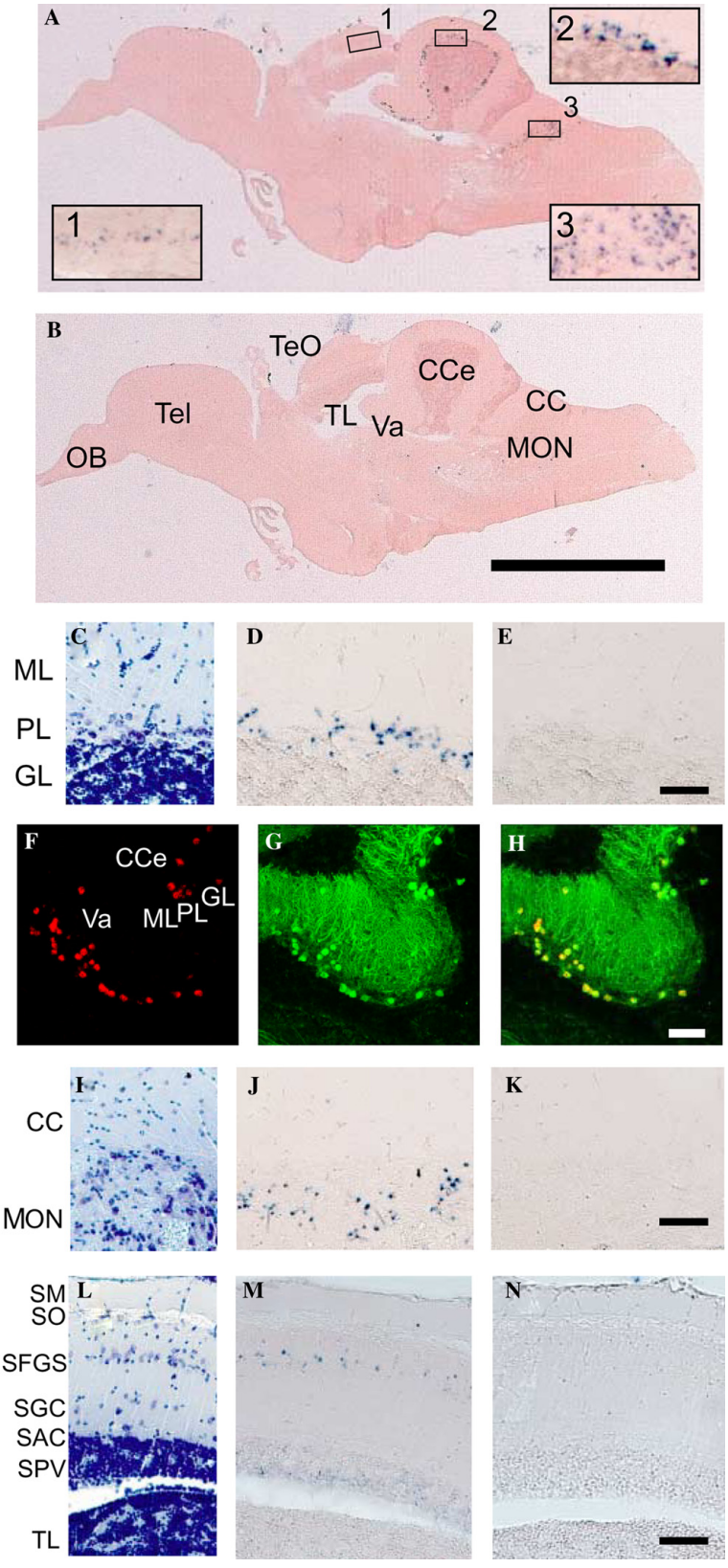

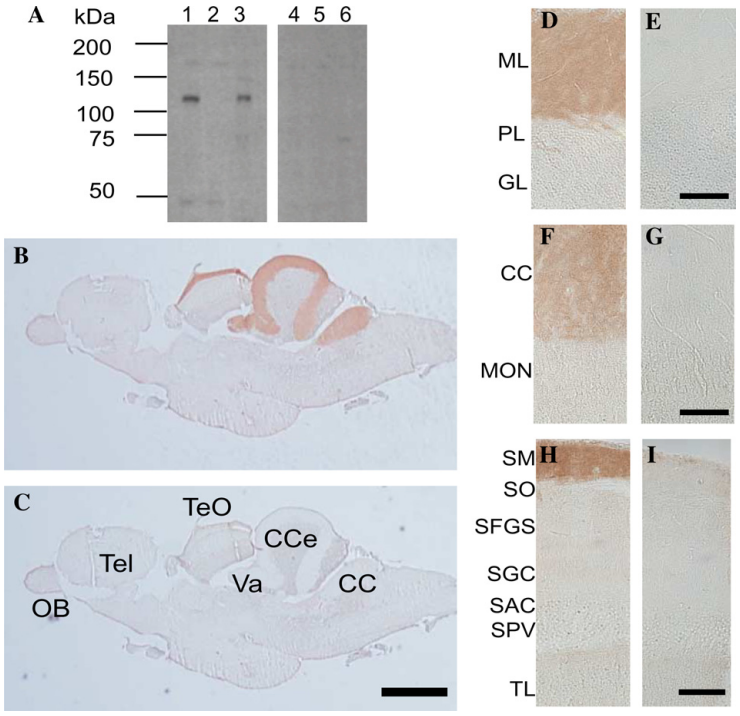

Fig. 3. Immunohistochemistry of GluRδ2 proteins in the adult zebrafish brain. (A) Western blot analysis of GluRδ2 proteins. Immunoblots of whole-brain homogenates from wild-type mice (lanes 1 and 4), mutant mice lacking GluRδ2 (lanes 2 and 5), and zebrafish (lanes 3 and 6) with anti-mouse GluRδ2 antibody (lanes 1–3) and GluRδ2-peptide-absorbed control antibody (lanes 4–6). The sizes of marker proteins are indicated to the left (kDa). A faint band (~75 kDa) is non-specific due to the second antibody. (B,C) Immunostaining of sagittal brain sections with anti-GluRδ2 (B) and GluRδ2-peptide-absorbed control (C) antibodies. GluRδ2 immunoreactivity was observed in the molecular layer of the cerebellum, the crista cerebellaris, and the stratum marginale of the optic tectum. CC, crista cerebellaris; CCe, corpus cerebelli; OB, olfactory bulb; Tel, telencephalon; TeO, optic tectum; and Va, valvula cerebelli. Scale bar, 500 μm. (D,E) Immunostaining of sagittal cerebellar sections with anti-GluRδ2 (D) and GluRδ2-peptide-absorbed control (E) antibodies. GluRδ2 immunoreactivity was observed in the molecular layer. ML, molecular layer; PL, Purkinje cell layer; and GL, granule cell layer. Scale bar, 50 μm. (F,G) Immunostaining of sagittal sections through the crista cerebellaris with anti-GluRδ2 (F) and GluRδ2-peptide-absorbed control (G) antibodies. GluRδ2 immunoreactivity was observed in the crista cerebellaris. CC, crista cerebellaris; MON, medial octavolateral nucleus. Scale bar, 50 μm. (H,I) Immunostaining of sagittal sections through the optic tectum with anti-GluRδ2 (H) and GluRδ2-peptide-absorbed control (I) antibodies. GluRδ2 immunoreactivity was observed in the stratum marginale layer. SM, stratum marginale; SO, stratum opticum; SFGS, stratum fibrosum et griseum superficiale; SGC, stratum griseum centrale; SAC, stratum album centrale; SPV, stratum periventriculare; and TL, torus longitudinalis. Scale bar, 50 μm.

Strong hybridization signals for *glurδ2* mRNA were present in the MON, but not in the crista cerebellaris (CC) (Figs. 2I–K). In the optic tectum, hybridization signals for *glurδ2* mRNA were found in the stratum fibrosum et griseum superficiale (SFGS) layer, but not in other five layers: the stratum marginale (SM), stratum opticum (SO), stratum griseum centrale (SGC), stratum album centrale (SAC), and stratum periventriculare (SPV) layers (Figs. 2L–N).

Localization of GluRδ2 proteins in neurons

Western blot analysis using anti-mouse GluRδ2 antibody showed a major immunoreactive band of about

Fig. 2. In situ hybridization analysis of the *glurδ2* mRNA in adult zebrafish brain with antisense and sense RNA probes. CC, crista cerebellaris; CCe, corpus cerebelli; and GL, granule cell layer. ML, molecular layer; MON, medial octavolateral nucleus; OB, olfactory bulb; PL, Purkinje cell layer; SAC, stratum album centrale; SFGS, stratum fibrosum et griseum superficiale; SGC, stratum griseum centrale; SM, stratum marginale; SO, stratum opticum; SPV, stratum periventriculare; Tel, telencephalon; TeO, optic tectum; TL, torus longitudinalis; and Va, valvula cerebelli. (A,B) Sagittal brain sections were labeled with antisense (A) and sense (B) riboprobes specific for zebrafish *glurδ2*. Hybridization signals (purple) were present in the cerebellum, the medial octavolateral nucleus, and the optic tectum. Higher magnification images of these regions are shown as insets. Scale bar, 1 mm. (C–E) Sagittal sections of the cerebellum. Sections were Nissl-stained (C), labeled with antisense (D), and sense (E) riboprobes specific for zebrafish *glurδ2*. Hybridization signals were observed in the Purkinje cell layer. Scale bar, 50 μm. (F–H) Double labeling of *glurδ2* mRNA and parvalbumin protein in the cerebellum. The *glurδ2* mRNA stained with HNPP/FastRed TR complex was imaged with a HeNe laser (F) and parvalbumin stained with avidin-Alexa Fluor 488 conjugate was imaged with an Ar laser (G). These images were merged on (H). Scale bar, 50 μm. (I–N) Sagittal sections of the medial octavolateral nucleus and crista cerebellaris (I–K) and optic tectum (L–N). Sections were Nissl-stained (I,L), labeled with antisense (J,M) and sense (K,N) riboprobes specific for zebrafish *glurδ2*, respectively. Hybridization signals were observed in the medial octavolateral nucleus (J) and the stratum fibrosum et griseum superficiale of the optic tectum (M). Scale bar, 50 μm.

120 kDa in whole-brain homogenates from zebrafish as well as from wild-type mice, but not from mutant mice lacking GluRδ2 (Fig. 3A). The anti-mouse GluRδ2 antibody was raised against the carboxyl-terminal segment of mouse GluRδ2 (amino acid residues 836–915; [5]) that is well conserved in zebrafish GluRδ2 (see above). Preabsorption of the anti-GluRδ2 antibody with mouse GluRδ2 peptide (residues 836–915) completely abolished the immunoreactivity of the 120 kDa band. We thus employed the rabbit anti-mouse GluRδ2 polyclonal antibodies for immunohistochemical analysis of zebrafish GluRδ2 and the preabsorbed antibodies as a negative control.

Immunohistochemical staining of sagittal sections of adult zebrafish brains showed GluRδ2 immunoreactivity in the cerebellar molecular layer, the CC, and the surface layer of the optic tectum (Figs. 3B and C). In the Va and CCe of the cerebellum, numerous immunoreaction products occupied the entire molecular layers (Figs. 3D and E). No staining signals were present in the Purkinje cell layer of the Va and CCe. These results suggest that GluRδ2 proteins are localized in the dendrites of Purkinje cells in the cerebellum.

The MON where *glurδ2* mRNA hybridization signals were localized showed no GluRδ2 immunoreactivity (Figs. 3F and G). Instead, strong immunostaining signals were found in the CC. Among three types of cells (crest cell, granule-like cell, and lateral interneuron) in the MON, the crest cell is the sole neuron that extends dendrites in the CC [33]. These results suggest that *glurδ2* mRNA expression in the MON can be assigned to crest cells and GluRδ2 proteins are localized in the dendrites of crest cells in the CC.

In the tectum, strong immunoreactive signals were localized in the stratum marginale (SM) layer (Figs. 3H and I), but not in the SFGS layer where *glurδ2* mRNA hybridization signals were localized. The SFGS layer contained the type I and type VI neurons [34]. Bipolar type I neurons in the SFGS layer extend the apical dendritic tree in the SM layer and basal dendritic trees in the SFGS and SGC layers. On the other hand, bipolar type VI neurons in the SFGS layer extend dendrites in the SO and SFGS layers and in the inner plexiform layer of SGC, but not in the SM layer [34]. Thus, we conclude that *glurδ2* mRNA expression in the SFGS layer of the tectum can be assigned to the type I neurons and GluRδ2 proteins are localized in the dendrites of the type I neurons in the SM layer.

Discussion

In the present investigation, we found that in the adult zebrafish brain, GluRδ2 is selectively expressed in the cerebellar Purkinje cells, the crest cells in the MON, and the type I neurons in the SFGS layer of the optic tectum. This expression profile of the zebrafish GluRδ2 appears to be in contrast with the very specific expression of mammalian GluRδ2 solely in the cerebellar Purkinje cells [5,6]. In the teleost as well as mammals, cerebellar Purkinje cells receive two excitatory inputs: very large numbers of weak inputs from parallel fibers and a single but strong input from climbing fiber [35–37]. Interestingly, the crest cells of the MON in the teleost octavolateralis system also receive two distinct excitatory inputs: large numbers of parallel fiber inputs from eminentia granularis (EG) on the apical dendrites in the CC and sensory inputs from the lateral line and eighth nerve end organ on the basal dendrites in the MON [36,38,39]. We have shown that GluRδ2 proteins are localized in the apical dendrites of

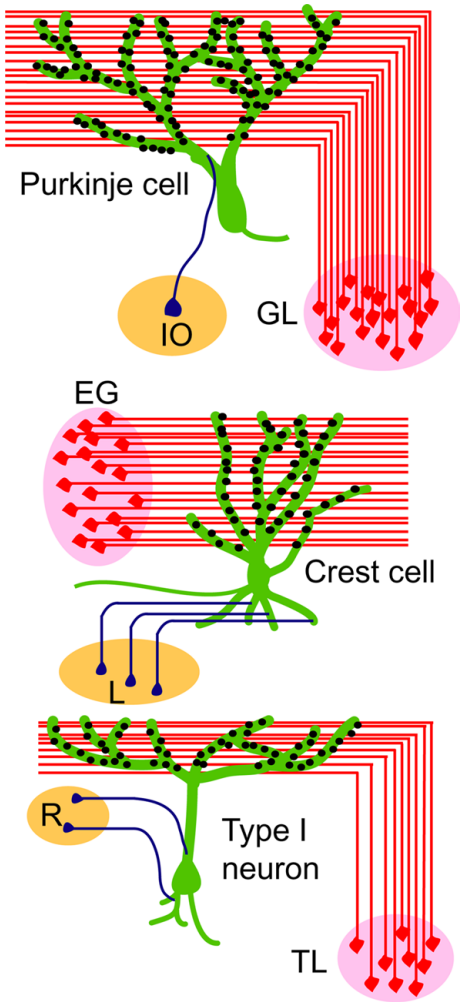

Fig. 4. Schematic diagram of wiring patterns of the cerebellar Purkinje cell (top), the crest cell of MON (middle), and the type I neuron of the optic tectum (bottom). These neurons have similar wiring patterns, receiving large numbers of parallel fiber inputs at the apical dendrites and climbing fiber or sensory inputs at the proximal or basal dendrites. Black circles on the apical dendrites of these neurons represent parallel fiber synapses. EG, eminentia granularis; GL, granule cell layer; IO, inferior olive; L, lateral line organ; R, retina; and TL, torus longitudinalis.

the crest cells in the CC, but not in the MON. Thus, GluRδ2 proteins are selectively localized in the apical dendrites of crest cells that receive large numbers of parallel fiber inputs from the EG. This selective localization pattern of GluRδ2 proteins in the crest cells is reminiscent of selective localization of mammalian GluRδ2 proteins at parallel fiber synapses in cerebellar Purkinje cells [7,8]. In the teleost optic tectum, the type I neurons also receive two distinct excitatory inputs: large numbers of parallel fiber inputs from the torus longitudinalis (TL) on the apical dendrites in the SM layer and sensory inputs from the retina onto the basal and proximal dendrites in the SFGS layer [36,39]. We have shown that GluRδ2 proteins are localized in the apical dendrites of the type I neurons in the SM layer, but not in the proximal and basal dendrites in the SFGS and SGC layers. Thus, GluRδ2 proteins are selectively localized again at the apical dendrites of the type I neurons that receive large numbers of parallel fiber inputs. These cerebellum-like structures are derived embryologically from the somatosensory portion of the alar plate and thus have common developmental origins [39]. Our findings show that in these specific types of neurons with similar characteristic wiring patterns, zebrafish GluRδ2 proteins are selectively localized at their apical dendrites that receive large numbers of parallel fiber inputs (Fig. 4).

Using GluRδ2 mutant mice, we have shown that GluRδ2 plays a key role in LTD of synaptic transmission at parallel fiber-Purkinje cell synapses [9]. Furthermore, decrease in the number of parallel fiber-Purkinje cell synapses and appearance of naked spines with no synaptic contacts in GluRδ2 mutant mice indicate that GluRδ2 is required for the stabilization of parallel fiber-Purkinje cell synapses [9,12]. In GluRδ2 mutant mice with decreased parallel fiber synapses, climbing fiber territory expanded distally along and beyond the target, resulting in persistent multiple climbing fiber innervation [9,14]. Thus, GluRδ2 was essential to restrict climbing fiber innervation to the proximal dendritic segment of the target Purkinje cell. These results suggest that GluRδ2 is essential for securing of the connection and territory of large numbers of weak parallel fiber inputs against a few but strong climbing fiber inputs. Thus, our findings that zebrafish GluRδ2 proteins are selectively localized at the apical dendrites of the crest cells in the MON and of the type I neurons in the optic tectum suggest that GluRδ2 may play a key role in cerebellum-like neural wiring with large numbers of parallel fiber inputs.

Acknowledgments

We thank Dr. Masahiko Watanabe for anti-GluRδ2 antibody. We are grateful to Dr. Ryo Kurita, Dr. Shinya Sato, and Dr. Sumiko Watanabe for helpful advice on in situ hybridization analysis and immunohistochemistry of zebrafish. This work was supported in part by research grants from the Japan Science and Technology Agency and the Ministry of Education, Culture, Sports, Science and Technology of Japan.

References

[1] M.L. Mayer, G.L. Westbrook, The physiology of excitatory amino acids in the vertebrate central nervous system, Prog. Neurobiol. 28 (1987) 197–276.
[2] M. Hollmann, S. Heinemann, Cloned glutamate receptors, Annu. Rev. Neurosci. 17 (1994) 31–108.
[3] M. Mishina, Molecular diversity, structure, and function of glutamate receptor channels, in: M. Endo, Y. Kurachi, M. Mishina (Eds.), Pharmacology of Ionic Channel Function: Activators and Inhibitors, Springer, Berlin, 2000, pp. 393–414.
[4] M. Yamazaki, K. Araki, A. Shibata, M. Mishina, Molecular cloning of a cDNA encoding a novel member of the mouse glutamate receptor channel family, Biochem. Biophys. Res. Commun. 183 (1992) 886–892.
[5] K. Araki, H. Meguro, E. Kushiya, C. Takayama, Y. Inoue, M. Mishina, Selective expression of the glutamate receptor channel δ2 subunit in cerebellar Purkinje cells, Biochem. Biophys. Res. Commun. 197 (1993) 1267–1276.
[6] H. Lomeli, R. Sprengel, D.J. Laurie, G. Köhr, A. Herb, P.H. Seeburg, W. Wisden, The rat delta-1 and delta-2 subunits extend the excitatory amino acid receptor family, FEBS Lett. 315 (1993) 318–322.
[7] C. Takayama, S. Nakagawa, M. Watanabe, M. Mishina, Y. Inoue, Developmental changes in expression and distribution of the glutamate receptor channel δ2 subunit according to the Purkinje cell maturation, Dev. Brain Res. 92 (1996) 147–155.
[8] A.S. Landsend, M. Amiry-Moghaddam, A. Matsubara, L. Bergersen, S. Usami, R.J. Wenthold, O.P. Ottersen, Differential localization of δ glutamate receptors in the rat cerebellum: coexpression with AMPA receptors in parallel fiber-spine synapses and absence from climbing fiber-spine synapses, J. Neurosci. 17 (1997) 834–842.
[9] N. Kashiwabuchi, K. Ikeda, K. Araki, T. Hirano, K. Shibuki, C. Takayama, Y. Inoue, T. Kutsuwada, T. Yagi, Y. Kang, S. Aizawa, M. Mishina, Impairment of motor coordination, Purkinje cell synapse formation, and cerebellar long-term depression in GluRδ2 mutant mice, Cell 81 (1995) 245–252.
[10] K. Funabiki, M. Mishina, T. Hirano, Retarded vestibular compensation in mutant mice deficient in δ2 glutamate receptor subunit, Neuroreport 7 (1995) 189–192.
[11] Y. Kishimoto, S. Kawahara, M. Suzuki, H. Mori, M. Mishina, Y. Kirino, Impairment of eyeblink conditioning in GluRδ2-mutant mice depends on the temporal overlap between conditioned and unconditioned stimuli, Eur. J. Neurosci. 14 (2001) 1515–1521.
[12] H. Kurihara, K. Hashimoto, M. Kano, C. Takayama, K. Sakimura, M. Mishina, Y. Inoue, M. Watanabe, Impaired parallel fiber → Purkinje cell synapse stabilization during cerebellar development of mutant mice lacking the glutamate receptor δ2 subunit, J. Neurosci. 17 (1997) 9613–9623.
[13] K. Hashimoto, R. Ichikawa, H. Takechi, Y. Inoue, A. Aiba, K. Sakimura, M. Mishina, T. Hashikawa, A. Konnerth, M. Watanabe, M. Kano, Roles of glutamate receptor δ2 subunit (GluRδ2) and metabotropic glutamate receptor subtype 1 (mGluR1) in climbing fiber synapse elimination during postnatal cerebellar development, J. Neurosci. 21 (2001) 9701–9712.
[14] R. Ichikawa, T. Miyazaki, M. Kano, T. Hashikawa, H. Tatsumi, K. Sakimura, M. Mishina, Y. Inoue, M. Watanabe, Distal

extension of climbing fiber territory and multiple innervation caused by aberrant wiring to adjacent spiny branchlets in cerebellar Purkinje cells lacking glutamate receptor δ2, J. Neurosci. 22 (2002) 8487–8503.
[15] K. Hironaka, H. Umemori, T. Tezuka, M. Mishina, T. Yamamoto, The protein-tyrosine phosphatase PTPMEG interacts with glutamate receptor δ2 and ε subunits, J. Biol. Chem. 275 (2000) 16167–16173.
[16] Y. Miyagi, T. Yamashita, M. Fukaya, T. Sonoda, T. Okuno, K. Yamada, M. Watanabe, Y. Nagashima, I. Aoki, K. Okuda, M. Mishina, S. Kawamoto, Delphilin: a novel PDZ and formin homology domain-containing protein that synaptically colocalizes and interacts with glutamate receptor δ2 subunit, J. Neurosci. 22 (2002) 803–814.
[17] T. Uemura, H. Mori, M. Mishina, Direct interaction of GluRδ2 with shank scaffold proteins in cerebellar Purkinje cells, Mol. Cell. Neurosci. 26 (2004) 330–341.
[18] J.S. Eisen, Zebrafish make a big splash, Cell 87 (1996) 969–977.
[19] T. Yoshida, A. Ito, N. Matsuda, M. Mishina, Regulation by protein kinase A switching of axonal pathfinding of zebrafish olfactory sensory neurons through the olfactory placode-olfactory bulb boundary, J. Neurosci. 22 (2002) 4964–4972.
[20] H. Tokuoka, T. Yoshida, N. Matsuda, M. Mishina, Regulation by glycogen synthase kinase-3β of the arborization field and maturation of retinotectal projection in zebrafish, J. Neurosci. 22 (2002) 10324–10332.
[21] T. Yoshida, M. Mishina, Neuron-specific gene manipulations in transparent zebrafish embryos, Methods Cell Sci. 25 (2003) 15–23.
[22] N. Guex, M.C. Peitsch, SWISS-MODEL and the Swiss-PdbViewer: an environment for comparative protein modeling, Electrophoresis 18 (1997) 2714–2723.
[23] T. Takahashi, D. Feldmeyer, N. Suzuki, K. Onodera, S.G. Cull-Candy, K. Sakimura, M. Mishina, Functional correlation of NMDA receptor ε subunits expression with the properties of single-channel and synaptic currents in the developing cerebellum, J. Neurosci. 16 (1996) 4376–4382.
[24] W. Hu, J. Zuo, P.L. De Jager, N. Heintz, The human glutamate receptor δ2 gene (GRID2) maps to chromosome 4q22, Genomics 47 (1998) 143–145.
[25] N. Ben-Arie, A.E. McCall, S. Berkman, G. Eichele, H.J. Bellen, H.Y. Zoghbi, Evolutionary conservation of sequence and expression of the bHLH protein Atonal suggests a conserved role in neurogenesis, Hum. Mol. Genet. 5 (1996) 1207–1216.
[26] J. Zuo, P.L. De Jager, K.A. Takahashi, W. Jiang, D.J. Linden, N. Heintz, Neurodegeneration in Lurcher mice caused by mutation in δ2 glutamate receptor gene, Nature 388 (1997) 769–773.
[27] Y. Stern-Bach, B. Bettler, M. Hartley, P.O. Sheppard, P.J. O'Hara, S.F. Heinemann, Agonist selectivity of glutamate receptors is specified by two domains structurally related to bacterial amino acid-binding proteins, Neuron 13 (1994) 1345–1357.
[28] I. Matsuda, M. Mishina, Identification of a juxtamembrane segment of the glutamate receptor δ2 subunit required for the plasma membrane localization, Biochem. Biophys. Res. Commun. 275 (2000) 565–571.
[29] S. Henikoff, J.G. Henikoff, Amino acid substitution matrices from protein blocks, Proc. Natl. Acad. Sci. USA 89 (1992) 10915–10919.
[30] P.J. O'Hara, P.O. Sheppard, H. Thøgersen, D. Venezia, B.A. Haldeman, V. McGrane, K.M. Houamed, C. Thomsen, T.L. Gilbert, E.R. Mulvihill, The ligand-binding domain in metabotropic glutamate receptors is related to bacterial periplasmic binding proteins, Neuron 11 (1993) 41–52.
[31] J.S. Sack, M.A. Saper, F.A. Quiocho, Periplasmic binding protein structure and function. Refined X-ray structures of the leucine/isoleucine/valine-binding protein and its complex with leucine, J. Mol. Biol. 206 (1989) 171–191.
[32] J.R. Alonso, R. Arèvalo, J.G. Briñòn, J. Lara, E. Weruaga, J. Aijòn, Parvalbumin immunoreactive neurons and fibres in the teleost cerebellum, Anat. Embryol. 185 (1992) 355–361.
[33] J.G. New, S. Coombs, C.A. McCormick, P.E. Oshel, Cytoarchitecture of the medial octavolateralis nucleus in the goldfish, *Carassius auratus*, J. Comp. Neurol. 366 (1996) 534–546.
[34] J. Meek, N.A. Schellart, A Golgi study of goldfish optic tectum, J. Comp. Neurol. 182 (1978) 89–122.
[35] T.E. Finger, Organization of the Teleost Cerebellum, in: R.G. Northcutt, R.E. Davis (Eds.), Fish Neurobiology, Vol. 1: Brain Stem and Sense Organ, The University of Michigan Press, Ann Abor, 1983, pp. 261–284.
[36] J. Meek, Why run parallel fibers parallel? Teleostean Purkinje cells as possible coincidence detectors, in a timing device subserving spatial coding of temporal differences, Neuroscience 48 (1992) 249–283.
[37] V.Z. Han, C.C. Bell, Physiology of cells in the central lobes of the mormyrid cerebellum, J. Neurosci. 23 (2003) 11147–11157.
[38] J. Montgomery, S. Coombs, R.A. Conely, D. Bodznick, Hindbrain sensory processing in lateral line, electrosensory, and auditory systems: a comparative overview of anatomical and functional similarities, Auditory Neurosci. 1 (1995) 207–231.
[39] C.C. Bell, Evolution of cerebellum-like structures, Brain Behav. Evol. 59 (2002) 312–326.